

Effects of Na/K evaporation on electrical properties and intrinsic defects in $\text{Na}_{0.5}\text{K}_{0.5}\text{NbO}_3$ ceramics

Laijun Liu^{a,b,c}, Huiqing Fan^{a,*}, Liang Fang^b, Xiuli Chen^a, Hichem Dammak^c, Mai Pham Thi^d

^a State Key Laboratory of Solidification Processing, School of Materials Science and Engineering, Northwestern Polytechnical University, Xi'an 710072, China

^b Key Laboratory of Nonferrous Materials and New Processing Technology, Ministry of Education, Guilin University of Technology, Guilin 541004, China

^c Laboratoire Structures, Propriétés et Modélisation des Solides, Ecole Centrale Paris, CNRS-UMR8580, Grande voie des Vignes, 92295, Châtenay-Malabry Cedex, France

^d Thales Research and Technology, Ceramics and Packaging Department, Domaine de Corbeville, 91404, Orsay, France

ARTICLE INFO

Article history:

Received 6 January 2009

Received in revised form 4 May 2009

Accepted 10 May 2009

Keywords:

Ceramics

Evaporation

Defects

Dielectric properties

ABSTRACT

The intrinsic defects of $(\text{Na}_{0.5}\text{K}_{0.5})\text{NbO}_3$ (NKN) ceramics fabricated by high-energy ball-milling have been studied. In order to obtain the different amounts of Na/K evaporation, NKN ceramics were sintered in air (NKN exposed samples) and in calcined NKN powder (NKN buried samples), respectively. Compared with the dielectric and piezoelectric properties of the buried samples, the exposed samples exhibited a donor doped behavior at room temperature. A dielectric relaxation, induced by intrinsic oxygen vacancies, was detected in paraelectric phase region. The activity energies of intrinsic oxygen vacancies are 1.04 eV and 1.47 eV for the exposed samples and buried samples, respectively. The difference of activity energies resulted from singly ionized oxygen vacancies translating into doubly ionized oxygen vacancies with the increase of Na/K evaporation.

© 2009 Elsevier B.V. All rights reserved.

1. Introduction

Sodium potassium niobium oxide, $\text{Na}_{0.5}\text{K}_{0.5}\text{NbO}_3$ (NKN) is a ferroelectric compound with the perovskite-type structure and is regarded as one of the promising compounds replacing the PZT materials which contain toxic Pb causing serious environment pollution [1,2]. $\text{Na}_{0.5}\text{K}_{0.5}\text{NbO}_3$ is well known to follow three phase transitions; rhombohedral to orthorhombic at 123 K; orthorhombic to tetragonal at 473 K and tetragonal to cubic at 693 K. Traditional sintered NKN ceramics may have electrical properties of piezoelectric constant, $d_{33} \sim 80$ pC/N; planar electromechanical coupling factor, $k_p \sim 36\text{--}40\%$; mechanical quality factor, $Q_m \sim 130$; and dielectric constant at room temperature, $\epsilon_r \sim 290$ [3]. However, the evaporations of Na_2O and K_2O during sintering at high temperatures prevent it from making high density and good performance. In order to improve the piezoelectric properties of NKN, hot presser sintering [4], sintering aids [5,6], control of stoichiometry [7,8], alkaline or rare earth elements doping [9–11] have been used to enhance their densification and control their microstructure.

The application of defect chemistry to fabricate electroceramics appears many years, which is based upon the fact that both sintering behavior and electrical properties can be influenced by ionic defects in ceramics. In $\text{PbZr}_x\text{Ti}_{1-x}\text{O}_3$ (PZT) ceramics, pure

(undoped) PZT has the intrinsic Pb vacancies induced by Pb evaporation during sintering at high temperatures [12–15]. Donors induce the Pb vacancies to maintain the charge neutrality. The increase of Pb vacancies can generate electrons by ionization; holes from Pb vacancies are compensated by electrons from the donor level to make ceramic resistivity increase with the addition of donor dopants. Therefore, the ceramics are easily poled due to higher resistivity. The dielectric constant of the ceramics is also improved with the increase of donor contents. Because the induced Pb vacancies in the lattice may minimize the local stresses and make the domain motions easier, the high mobility of domain walls leads to an increase in dielectric loss and a decrease in mechanical quality factor [15]. Up to now, however, the influence of the type and concentration of defects on piezoelectric and dielectric properties of NKN ceramics is not clear.

In this work, two kinds of sintering methods were used to bring the different amounts of intrinsic Na/K vacancies. Dielectric properties as functions of temperature and frequency carried out on NKN ceramics using an impedance analyzer are described. A Debye-like dielectric relaxation was observed in both NKN exposed samples and buried samples in paraelectric phase region. Their respective data were analyzed by the semiempirical complex Cole–Cole equation. At the same time, we also showed the effect of intrinsic Na/K vacancies on the piezoelectric properties of NKN ceramics. The results were discussed in light of inadvertent Na_2O and K_2O evaporation induced off-stoichiometric oxygen vacancies in NKN ceramics.

* Corresponding author.

E-mail addresses: ljliu2@163.com (L. Liu), hqfan3@163.com (H. Fan).

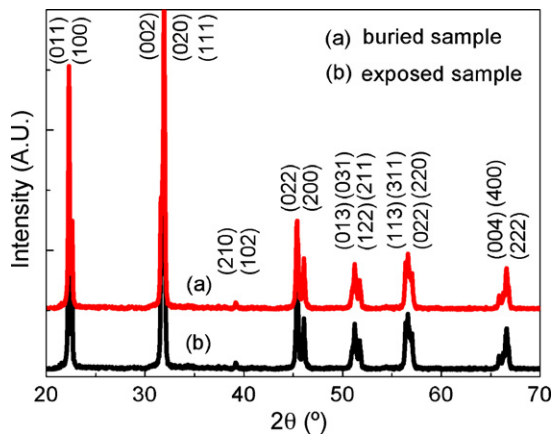


Fig. 1. XRD patterns of NKN exposed samples and NKN buried samples.

2. Experiment

Carbonates and oxides Na_2CO_3 (PROLABO, 99.9%), $\text{K}_2\text{CO}_3 \cdot 1.5\text{H}_2\text{O}$ (MERCK, 99.995%) and Nb_2O_5 (INTERCHIM, 99.5%) were used as starting materials. Retsch mill (PM 100) was used for mechanical alloying to fabricate NKN powder. Perovskite NKN powder was obtained after milling 450 rpm for 2 h and then calcined at 850°C for 2.5 h. The calcined powder was pressed into discs uniaxially of 10 mm in diameter and 2 mm in thickness under 300 MPa and then pressed under 650 MPa with a cool isostatic pressing method. In order to obtain different off-stoichiometric vacancy defects, one group of discs was buried in calcined NKN powder (NKN buried samples), and the other group of discs was exposed in air (NKN exposed samples). Both of them were sintered in an alumina crucible at 1090°C for 4 h.

X-ray diffraction patterns were obtained using an automated diffractometer (XRD; SIEMENS D5000) with $\text{Cu K}\alpha_1$ radiation. Both sides of the samples were sputtered gold electrodes. A poling treatment was conducted using a DC power supply at 2.5 kV mm^{-1} in castor oil at 160°C for 10 min then cooling with the electrical field. Electrical properties measurement were taken with an applied voltage of 500 mV over the frequency range 40 Hz to 5 MHz from 350 K to 830 K with an impedance analyzer (Agilent 4294A). The resonance–anti-resonance frequency of them should be tested to detect piezoelectric properties, which were obtained using the following equations:

$$\frac{1}{k_p^2} = 0.395 \frac{f_R}{f_A - f_R} + 0.574 \quad (1)$$

$$Q_m = \frac{1}{2\pi f_R R_1 C_f [1 - (f_R/f_A)^2]} \quad (2)$$

$$N_p = f_R d \quad (3)$$

$$s_{11} = \frac{\eta^2}{(1 - \sigma^2)(\pi d f_r)^2 \rho} \quad (4)$$

$$k_{31} = \left(\frac{1 - \sigma}{2}\right)^{1/2} k_p \quad (5)$$

where f_R is resonance frequency, f_A is anti-resonance frequency, Q_m is mechanical quality factor, R_1 is the impedance at resonance frequency, C_f is the capacitance at 1 kHz, N_p is resonance frequency constant, d is the diameter of sample, s_{11} is elastic compliance and ρ is the density of samples, k_p is planar electromechanical coupling factor, k_{31} is lateral electromechanical coupling factor, σ is Poisson ratio.

3. Results and discussion

XRD patterns of NKN buried and NKN exposed samples are shown in Fig. 1. The recorded patterns match very well with JCPDS card 32-0822, which indicates that the sintered samples exhibit a single phase. The Bragg reflections were easily indexed to the orthorhombic crystal system with $Amm2$ space group. We cannot find the obvious difference or superlattice reflections for NKN buried and NKN exposed samples in XRD patterns. The densities, 4.20 g cm^{-3} and 4.03 g cm^{-3} are corresponding to NKN buried and exposed samples, respectively. The lattice parameter of NKN ceramics was also calculated according to their XRD patterns: $a = 3.943\text{ \AA}$, $b = 5.642\text{ \AA}$ and $c = 5.675\text{ \AA}$ for NKN buried sample, and $a = 3.942\text{ \AA}$, $b = 5.640\text{ \AA}$ and $c = 5.671\text{ \AA}$ for NKN exposed sample. Cell volumes of

NKN buried and exposed samples are 126.248 \AA^3 and 126.083 \AA^3 , respectively, which suggests that Na/K evaporation results in a decrease of density and cell volumes.

The temperature dependence of the dielectric constant and dielectric loss at 1 kHz during heating for NKN ceramics is shown in Fig. 2. Three dielectric anomalies can be found for poled NKN buried and exposed ceramics. Two of them, corresponding to the phase transitions from orthorhombic to tetragonal and from tetragonal to cubic, present at 450 K and 650 K, respectively; the third presents at 520 K corresponding to the depolarization process of NKN ceramics. However, the depolarization temperatures of them are much lower than NKN Curie temperature, which is similar to A-site complex compound $\text{Na}_{0.5}\text{Bi}_{0.5}\text{TiO}_3$ based solid solution [17]. The great difference between depolarization temperature and Curie temperature may result from an incomplete poling process because the domain of NKN ceramics has not switched completely during poling. As seen in Fig. 2, NKN buried samples exhibit a higher dielectric constant and dielectric loss compared with that of NKN exposed samples in high temperature, but it looks like contrary in low temperature. On the other hand, NKN exposed samples have not a clear dielectric constant peak during depolarization process. Only a weak depolarization peak is observed at 520 K in the plot of temperature dependence of dielectric loss factor for NKN exposed samples. The difference of polarization behavior results from the interaction of domain among lattice and defect structure.

A comparison of dielectric and piezoelectric properties of NKN ceramics, which are obtained by different processing routes, is shown in Table 1. The dielectric constant and loss factor and elastic coefficient of NKN exposed samples are higher than those of NKN buried samples, and the mechanic quality factor, electromechanical coupling factor are less than those of NKN buried samples. It is considered that NKN exposed samples exhibit a donor doped behavior compared with NKN buried samples. The cation vacancies can minimize the local stresses in lattice and make the domain motions easier [12–15], which leads to increases in dielectric constant and loss factor and a decrease in mechanical quality factor. This also provides a possible explanation that the dielectric properties of NKN exposed samples are higher than those of NKN buried samples at room temperature (Table 1). However, the dielectric constant of NKN buried samples is higher than that of NKN exposed samples in high temperature, which suggests that hopping carrier or/and oxygen vacancies make great influence on the dielectric properties in NKN ceramics.

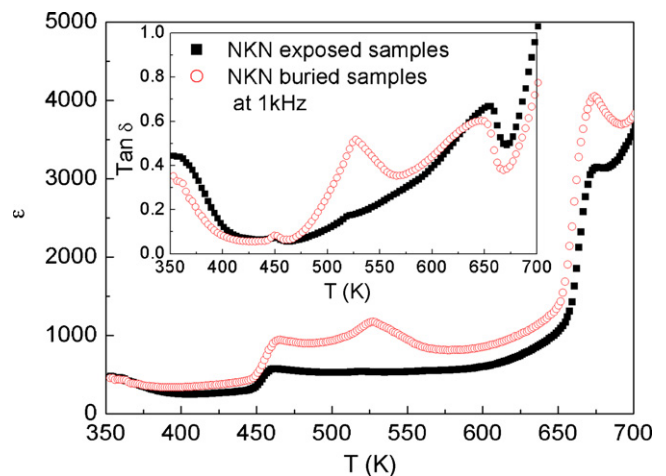


Fig. 2. Real part of dielectric constant and loss tangent curves as a function of temperature at 1 kHz for NKN exposed samples and NKN buried samples. The samples are poled and the data recorded during heating.

Table 1
Comparison of electrical properties of NKN obtained by different groups.

Properties	NKN exposed this study	NKN buried this study	Jaeger and Egerton NKN [16] air-sintered	Kosec and Kolar, NKN [11] air-sintered	Birol et al. NKN [18] air-sintered	Jaeger and Egerton hot-pressed NKN [16]
ε (1 kHz)	472	453			472	
$\tan \delta$ (1 kHz)	0.44	0.35				
k_p	0.29	0.34	0.36	0.23	0.39	0.45
Q_m	12	50				
σ_{12}	0.27	0.31	0.27		0.33	0.27
k_{31}	0.27	0.31	0.22		0.23	0.27
N_ϕ (Hz m)	3073	3233				
S_{11} ($\text{m}^2 \text{kg}^{-1}$)	6.5×10^{-12}	5.9×10^{-12}			8.7×10^{-12}	
d_{31} (pC/N)	38.7	46.2	32		43.4	49

Generally, intrinsic cation vacancies associate with oxygen vacancies in perovskite compound in order to maintain the charge neutrality. Oxygen vacancies coagulate with the intrinsic cation vacancies to build an internal space charge in ferroelectric, which restricts the motion of domain. Here, impedance spectroscopy (40 Hz to 1 MHz) is used to analyse the characteristic of the oxygen vacancies. The complex impedance can be expressed in terms of the real and imaginary components Z' and Z'' :

$$Z = Z' + jZ'' = |Z| \exp j\theta^{-1} \quad (6)$$

where, $|Z|$ and θ are the magnitude and the phase of the impedance, respectively. Cole–Cole plots above NKN Curie temperature were recorded, which are shown in Fig. 3. In order to eliminate the effect of size of samples, the real part and imaginary part of impedance were multiplied by the area and divide by the thickness of samples. NKN exposed samples (Fig. 3a) and NKN buried samples (Fig. 3b)

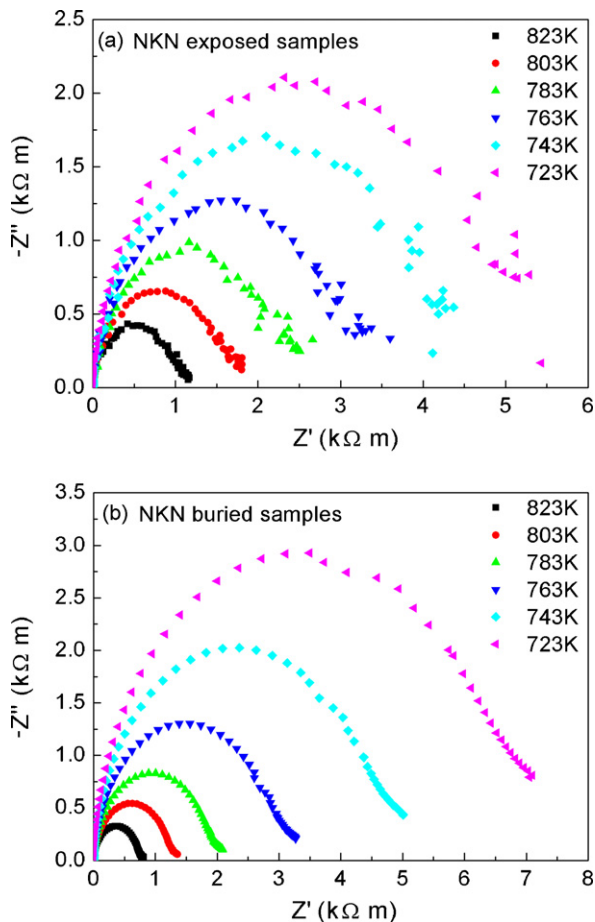


Fig. 3. Impedance complex plane plot, Z'' at different temperatures. (a) NKN exposed samples and (b) NKN exposed samples.

have similar relaxation behavior in paraelectric phase region. The relaxation frequency (ω) at the apex of the Cole–Cole semicircle, is an intrinsic characteristic frequencies of NKN ceramics, and fulfills the condition $\omega RC = 1$. The activation energies of the aforementioned electrical responses from relaxation times ($\omega = 1/\tau$) are calculated. Relaxation frequencies are obtained, and plotted against reciprocal temperature in Arrhenius format:

$$\omega = \omega_0 \exp\left(\frac{-E_a}{k_B T}\right) \quad (7)$$

where ω_0 is the preexponential factor, E_a is the activation energy for the relaxation, k_B is the Boltzmann constant, and T is the absolute temperature. Fig. 4 shows the plot of $\ln \omega$ versus $1/T$, in which the solid line is fitted by Eq. (7). Both of them obey the Arrhenius law with activation energies of 1.04 eV for NKN exposed samples and 1.47 eV for NKN buried samples. The preexponential factors ω_0 are 2.0×10^{11} and 3.5×10^{14} , corresponding to NKN exposed samples and NKN buried samples, respectively. The difference of preexponential factor should be caused by the type and concentration of oxygen vacancy.

Generally, the origin of the dielectric relaxation arises from the motion of the domain walls, long-range disorders, interfacial polarization, carrier hopping, and the thermal motion of ions to different sites. However, why do we confirm this dielectric relaxation is caused by oxygen vacancies here? Dielectric relaxation in $\text{Ba}(\text{Ti}_x\text{Zr}_{1-x})\text{O}_3$ is attributed to long-range disorder and the activation energy is ~ 0.5 eV.[19] The activation energy is associated with the height of the potential-energy barrier restricting the motion of charge carriers, but activation energies in the present work are more than 1 eV. The dielectric relaxation in Bi-doped SrTiO_3 [20], doped BaTiO_3 [21], and Ca-doped $\text{KTa}_{1-x}\text{Nb}_x\text{O}_3$ [22] is associated with defect-induced relaxations, but our compound is pure NKN. Furthermore, it is not also a domain wall relaxation because our

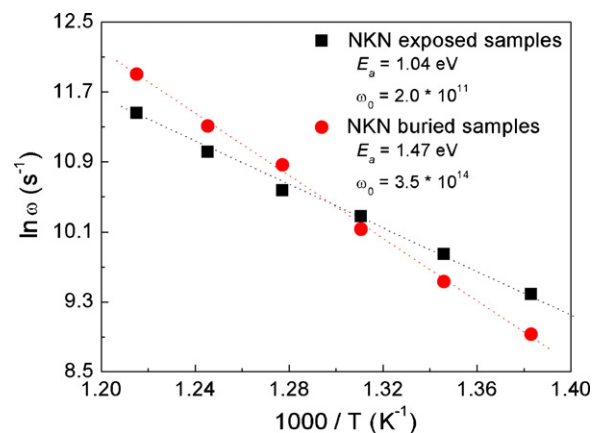


Fig. 4. Arrhenius plot for relaxation frequency in the temperatures between 723 K and 823 K. The solid line through the data is a linear fit to Eq. (7).

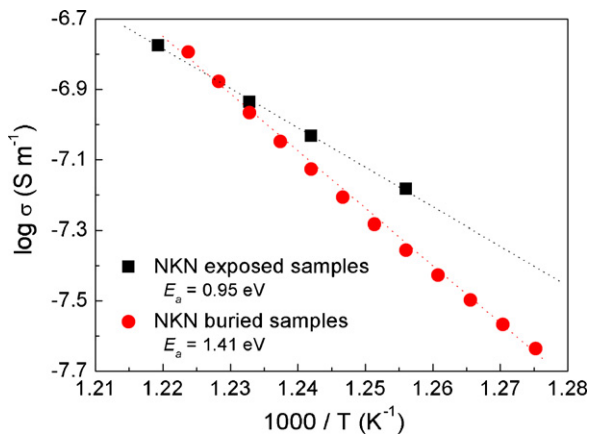
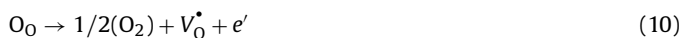


Fig. 5. Arrhenius plot for ions hopping conductivity in paraelectric region. The solid line through the data is a linear fit to Arrhenius equation.

relaxation presents in paraelectric region. On the other hand, the short arcs in low frequency may correspond to Maxwell–Wagner or interfacial polarizations in Fig. 3, so it is also not an interfacial relaxation. Computational simulations of the ionic transport in perovskite oxides indicate that the activation energy for oxygen vacancy migration is around 1 eV, for the A-site cation transport is around 4 eV, and for the B-site cation migration is around 14 eV [23]. We also analyze the temperature dependence of ac conductivity and obtain the activation energies of ions hopping conduction (shown in Fig. 5), 0.95 eV and 1.41 eV for NKN exposed samples and NKN buried samples, respectively. These activation energies match well for the oxygen vacancy migration. Consequently, the oxygen vacancy play important role on the ions hopping conduction in NKN ceramics at high temperatures.

However, NKN exposed and buried samples have different activation energies for hopping frequency, 1.04 eV and 1.47 eV, respectively. The difference should be caused by the differences of concentration and type of oxygen vacancy.

The sodium/potassium oxide evaporation results in a nonstoichiometry, and the defect structure can be written as:



The concentration of the sodium/potassium vacancies, V'_{Na} or V'_{K} , would be double that of one or two oxygen vacancy(s), $V^{\bullet}_{\text{O}}/V^{\bullet\bullet}_{\text{O}}$ [24]. The Na/K evaporation makes a weight loss and corresponds to a loss of oxygen from NKN ceramics. Cronemeyer [25] pointed out an oxygen vacancy can be seen as a doubly charged positive center capable of trapping two electrons, that the ionization energy for the first electron will be that of a helium atom immersed in a dielectric medium. And the ionization energy is 0.73 eV. Moreover, if one electron is ionized form an oxygen vacancy, it is should be possible to observe a second ionization energy of 1.64 eV. With the increase of Na/K evaporation, there must be a transition from singly ionized oxygen vacancies to doubly ionized oxygen vacancies, as the concentration of such oxygen vacancies increase. So

the decrease of thermal ionization energy accompanies an increase of oxygen vacancy concentration. Such a decrease in ionization energy attributed to interaction of the individual donor centers when closed spaced is a well-known feature of the standard semiconductors [26].

NKN is one of the important candidate materials for environmental friendly piezoelectric ceramics. Polarization process is necessary for the piezoelectric tests and applications. The cation vacancies and oxygen vacancies play important role on the electrical properties. Consequently, sintering process and donor/acceptor doped can be used to change the defect characteristic and improve the performance of NKN ceramics according to its application field.

4. Conclusions

The effects of Na/K evaporation on electrical properties and the activation energy of oxygen vacancies in NKN ceramics were investigated. NKN exposed sample exhibits a donor doped behavior compared NKN buried samples for the piezoelectric properties at room temperature. The oxygen vacancy plays important role on the ions hopping conduction of NKN ceramics at high temperatures. The activation energy of oxygen vacancies for NKN exposed samples is lower than that for NKN buried samples. The increase of Na/K evaporation accompanies an increase in the concentration of oxygen vacancies, which leads to a transition from singly ionized oxygen vacancies to doubly ionized oxygen vacancies.

Acknowledgements

This work was supported by the National Nature Science Foundation (50672075), the SRFDP (20050699011) and NCET Program and 111 Project (B08040) of MOE, the Fundamental Research Foundation (NPU-FFR-200703) and Doctorate Foundation (CX200704) of NPU of China.

References

- [1] Y.P. Guo, K. Kakimoto, H. Ohsato, *Solid State Commun.* 129 (2004) 279–284.
- [2] M. Matsubara, K. Kikuta, S. Hirano, *J. Appl. Phys.* 97 (2005) 114105.
- [3] L. Egerton, D.M. Dillon, *J. Am. Ceram. Soc.* 42 (1959) 438.
- [4] G.H. Haertling, *J. Am. Ceram. Soc.* 50 (1967) 329.
- [5] R.Z. Zuo, J. Rodel, R.Z. Chen, L.T. Li, *J. Am. Ceram. Soc.* 89 (2006) 2010.
- [6] S.H. Park, C.W. Ahn, S. Nahm, J.S. Song, *Jpn. J. Appl. Phys.* 43 (2004) L1072.
- [7] Z.S. Ahn, W.A. Schulze, *J. Am. Ceram. Soc.* 70 (1987), C-18.
- [8] J. Yoo, K. Lee, K. Chung, S. Lee, K. Kim, J. Hong, S. Ryu, C. Lhee, *Jpn. J. Appl. Phys.* 45 (2006) 7444.
- [9] B. Malic, J. Bernard, J. Holc, D. Jenko, M. Kosec, *J. Eur. Ceram. Soc.* 25 (2005) 2707.
- [10] S.N. Murty, K. Umarantham, A. Bhanamathi, *Ferroelectrics* 82 (1988) 141.
- [11] M. Kosec, D. Kolar, *Mater. Res. Bull.* 10 (1975) 335.
- [12] X. Dai, Z. Xu, D. Viehland, *J. Am. Ceram. Soc.* 78 (1995) 2815–2823.
- [13] P.G.R. Lucuta, F.L. Constantinescu, D. Barb, *J. Am. Ceram. Soc.* 68 (1985) 533.
- [14] M. Pereira, A.G. Peixoto, M.J.M. Gomes, *J. Eur. Ceram. Soc.* 21 (2001) 1353.
- [15] C. Miclea, C. Tanasoiu, C.F. Miclea, L. Amarande, A. Gheorghiu, F.N. Sima, *J. Eur. Ceram. Soc.* 25 (2005) 2397.
- [16] R.E. Jaeger, L. Egerton, *J. Am. Ceram. Soc.* 45 (1962) 209–213.
- [17] B. Chu, D. Chen, G. Li, Q. Yin, *J. Eur. Ceram. Soc.* 22 (2002) 2115.
- [18] H. Birol, D. Damjanovic, N. Setter, *J. Eur. Ceram. Soc.* 26 (2006) 861–866.
- [19] Z. Yu, R. Guo, A.S. Bhalla, *J. Appl. Phys.* 88 (2000) 410.
- [20] C. Ang, Z. Yu, L.E. Cross, *Phys. Rev. B* 62 (2000) 228.
- [21] R. Stumpe, D. Wagner, *Phys. Status Solidi A* 75 (1983) 143–154.
- [22] G.A. Samara, L.A. Boatner, *Phys. Rev. B* 61 (2000) 3889.
- [23] M.S. Islam, *J. Mater. Chem.* 10 (2000) 1027.
- [24] W.S. Lau, T. Han, *Appl. Phys. Lett.* 86 (2005) 152107.
- [25] D.C. Cronemeyer, *Phys. Rev.* 113 (1959) 1222.
- [26] G.L. Pearson, J. Bardeen, *Phys. Rev.* 75 (1949) 865.